

Clinical Article

Engraftment of Human Mesenchymal Stem Cells in a Rat Photothrombotic Cerebral Infarction Model : Comparison of Intra-Arterial and Intravenous Infusion Using MRI and Histological Analysis

Jun Soo Byun, M.D., Ph.D., Byung Kook Kwak, M.D., Ph.D., Jae Kyun Kim, M.D., Jisung Jung, M.S., Bon Chul Ha, M.S., Serah Park, B.S.

Department of Radiology, Chung-Ang University College of Medicine, Seoul, Korea

Objective : This study aimed to evaluate the hypotheses that administration routes [intra-arterial (IA) vs. intravenous (IV)] affect the early stage migration of transplanted human bone marrow-derived mesenchymal stem cells (hBM-MSCs) in acute brain infarction.

Methods : Male Sprague-Dawley rats (n=40) were subjected to photothrombotic infarction. Three days after photothrombotic infarction, rats were randomly allocated to one of four experimental groups [IA group : n=12, IV group : n=12, superparamagnetic iron oxide (SPIO) group : n=8, control group : n=8]. All groups were subdivided into 1, 6, 24, and 48 hours groups according to time point of sacrifice. Magnetic resonance imaging (MRI) consisting of T2 weighted image (T2WI), T2* weighted image (T2*WI), susceptibility weighted image (SWI), and diffusion weighted image of rat brain were obtained prior to and at 1, 6, 24, and 48 hours post-implantation. After final MRI, rats were sacrificed and grafted cells were analyzed in brain and lung specimen using Prussian blue and immunohistochemical staining.

Results : Grafted cells appeared as dark signal intensity regions at the peri-lesional zone. In IA group, dark signals in peri-lesional zone were more prominent compared with IV group. SWI showed largest dark signal followed by T2*WI and T2WI in both IA and IV groups. On Prussian blue staining, IA administration showed substantially increased migration and a large number of transplanted hBM-MSCs in the target brain than IV administration. The Prussian blue-positive cells were not detected in SPIO and control groups.

Conclusion : In a rat photothrombotic model of ischemic stroke, selective IA administration of human mesenchymal stem cells is more effective than IV administration. MRI and histological analyses revealed the time course of cell migration, and the numbers and distribution of hBM-MSCs delivered into the brain.

Key Words : MRI · Mesenchymal stem cell · Photothrombotic cerebral infarction · Superparamagnetic iron oxide · Intravascular.

INTRODUCTION

Human bone marrow-derived mesenchymal stem cells (hBM-MSCs) transplantation following experimental stroke promotes functional recovery in animal models^{39,66,67}. The transplanted may potentially mediate recovery through differentiation into functional neuronal cells (microglia, new neural stem cells, neurons, oligodendrocytes, and astrocytes)^{10,46,63,65}, induction of neurogenesis^{14,57}, synapse formation (synaptogenesis)⁵⁵, and neuroprotection (inhibition of apoptosis, inflammation and demyelination while promoting astrocyte survival)^{13,39,40,56}. By promoting angiogenesis¹⁵, the hBM-MSCs may help to restore

cerebral blood flow and the blood brain barrier^{8,9}. Perhaps underlying these diverse mechanisms is the capacity of hBM-MSC to promote endogenous repair and regeneration through induction of cytokines and trophic factors such as brain-derived neurotrophic factor, insulin-like growth factor-1, nerve growth factor, fibroblast growth factor-2, vascular endothelial growth factor and stromal cell-derived factor-1 (SDF-1)^{8,13,16,17,20,40,56}.

The route chosen for delivery of cells may influence the migration and final destination of the transplanted cells. Direct intracerebral^{26,29}, intravascular^{13,15,18,55,59}, intrathecal⁴¹, and intraventricular³² delivery of cells for transplantation have been tested. Intravascular delivery presents such advantages as safety and

• Received : February 22, 2013 • Revised : July 17, 2013 • Accepted : December 12, 2013

• Address for reprints : Byung Kook Kwak, M.D., Ph.D.

Department of Radiology, Chung-Ang University Hospital, 102 Heukseok-ro, Dongjak-gu, Seoul 156-755, Korea
Tel : +82-2-6299-2661, Fax : +82-2-6263-1557, E-mail : kwakbk@cau.ac.kr

• This is an Open Access article distributed under the terms of the Creative Commons Attribution Non-Commercial License (<http://creativecommons.org/licenses/by-nc/3.0>) which permits unrestricted non-commercial use, distribution, and reproduction in any medium, provided the original work is properly cited.

wide distribution of stem cells within the ischemic penumbra as compared to other method. Intravascular transplantation may proceed by either intra-arterial (IA) or intravenous (IV) delivery. Experimentally, the IV^{13,15,18}, and IA^{55,59} routes have been used to investigate homing capabilities and mechanisms of the MSCs, and to show that IV administration results in greater cell trapping by systemic organs such as lung, liver, spleen than IA injection. These observations may be relevant to achieving therapeutic densities of hBM-MSCs in a rat's photothrombotic cerebral infarction model^{22,47}. IA administration of stem cells to the injured or ischemic brain may be significantly more effective in achieving delivery of cells than by the IV route^{26,38,42}. Previous studies have demonstrated that IA administration of stem cells to the injured brain or ischemic brain was significantly more effective than the IV route, however, there was no study that showed MRI and pathologic correlation analysis. In present study, we evaluated the migration and distribution of hBM-MSCs transplanted by IA and IV injection routes into the photothrombotic cerebral infarction region of the rat during 48 hours after cell transplantation (5 days after infarction). Here, we present the magnetic resonance imaging (MRI) and pathologic analyses performed in parallel with the treatment.

MATERIALS AND METHODS

Ethical statement

Rats were maintained in accordance with guidelines of the Institutional Animal Ethics Committee at our institution. The Institutional Review Board of CAUH (CAUMD 11-0020) approved this study.

Cell culture and labeling

Adult bone marrow contains two types of prototypical stem cells, the hematopoietic and the MSCs²¹. Also referred to as bone marrow stromal cells, the MSC may under specific conditions differentiate into osteocytes, chondrocytes, adipocytes, and myocytes^{7,33}. MSCs may alternatively differentiate into neuronal cells, including astrocytes, neurons, and endothelial cells in the brain^{1,23,43}. We used commercially available hBM-MSC (HMSC-bm #7500; ScienCell Research Laboratories, Carlsbad, CA, USA) that were isolated from human bone marrow. The cells were confirmed to express the CD 13, 29, 44, 73, 90, 105, and 106 surface antigen and to lack CD 14, 34, 106, and 133 expression.

The hBM-MSC were cultured in a humidified atmosphere with 5% CO₂ at 37°C in Dulbecco's modified Eagle's medium (DMEM; Invitrogen, Carlsbad, CA, USA) that was supplemented with 10% fetal bovine serum, 200 mM L-glutamine, 1%

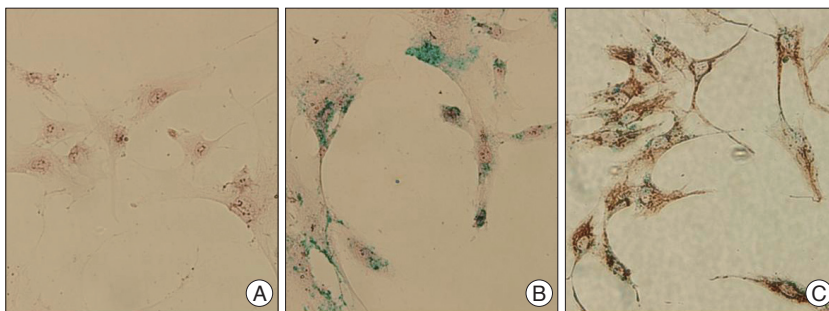


Fig. 1. *In vitro* cell staining. A : Non-labeled human mesenchymal stem cell, Prussian blue staining, original magnification $\times 400$. B : Labeled hMSC, Prussian blue staining, original magnification $\times 400$. C : Combined staining with antimitochondrial antibody-Prussian, original magnification $\times 400$.

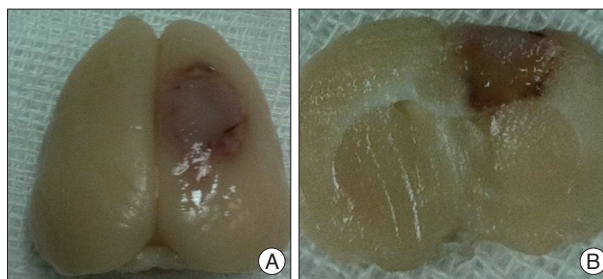


Fig. 2. Rat brain 5 days after photothrombotic infarction in right frontoparietal lobes. Whole cerebrum of rat brain (A) and coronal cross section (B).

penicillin and streptomycin. The medium was replaced every 3 days and the cells were sub-cultured at 80-90% growth confluence. Cells were labeled overnight with superparamagnetic iron oxide (SPIO) nanoparticles.

We used a clinically approved SPIO (Feridex IV, ferumoxide; Advanced Susceptibility Inc., Cambridge, MA, USA). The SPIO are characterized by a 5-nm iron core and hydrodynamic diameter of 80-90 nm, including the dextran coating⁵¹. Ferumoxide is provided as an SPIO solution with a total iron content of 11.2 mg/mL and is approved for clinical use in liver imaging. By reducing the transverse relaxation time (T₂) on T₂-weighted images, the SPIO nanoparticles cause labeled cells to appear as regions of dark signal intensity. To facilitate endocytosis of SPIO by the hBM-MSCs, the polyamine poly-L-lysine hydrobromide (PLL; Sigma-Aldrich Corp., St. Louis, MO, USA) was used³⁷. To obtain a final PLL concentration of 375 ng/mL and 25 μ g/mL of SPIO in the medium, the PLL at 750 ng/mL and SPIO at 50 μ g/mL were mixed with culture medium and gently shaken for 60 minutes at room temperature. The hBM-MSCs were labeled with SPIO by incubation overnight in medium containing SPIO-PLL complex at 37°C in a 5% CO₂ humidified atmosphere. The viability of the SPIO-labeled hBM-MSCs before transplantation was assessed at greater than 85% by trypan blue exclusion. Before injection into rats, the labeled cells were prepared in phosphate-buffered saline (PBS). Nearly 100% labeling of hBM-MSCs with SPIO was achieved, as shown by Prussian blue and immunohistochemical staining, and cellular MRI performed *in vitro* (Fig. 1A, B). Mitochondria and iron were detected in the hBM-MSC by combined staining with anti-mito-

chondrial antibody and Prussian blue (Fig. 1C).

Photothrombotic infarction model

Photothrombotic infarction was induced in 40 male Sprague-Dawley rats (250-280 g). Anesthesia was induced with 5% isoflurane (Aerane Solution; Ilsung-medicine, Seoul, Korea) in O₂, and maintained with 1.5-2% isoflurane by inhalation. The rat was placed in supine position on the table and its head was fixed to a stereotactic system (Stoelting Co., Wood Dale, IL, USA). The skull was exposed by a scalp incision along the midline and an optical fiber guide from the cold light generator (Fiber-Lite MI-150; Dolan-Jenner Industries, Inc., Boxborough, MA, USA) with a 5-mm aperture was positioned onto the skull 2.5 mm right lateral to the midline and 2.5 mm posterior to the bregma. Wavelength of the light was 400-670 nm, and its color temperature was 3200°K. After intravenous injection of the photosensitive Rose Bengal (20 mg/kg, Sigma-Aldrich Co., St. Louis, MO, USA) through the tail vein, photoillumination was performed for 15 minutes. Focal activation of the photosensitive Rose Bengal induces free-radical injury to endothelial cells, platelet aggregation leading to microvascular thrombosis and occlusion of the vessel, causing circumscribed cortical infarctions⁶². The scalp was sutured with 4-0 blue-nylon and rats were allowed to wake up from the anesthesia. During the procedure, the rectum temperature of rats was monitored with a homeothermic blanket control unit (Harvard Apparatus, Holliston, MA, USA) and maintained between 36.5 and 37°C with a feedback-controlled heating pad. Photothrombotic infarction was successfully induced in all of the experimental rats. The location of infarction was the right frontoparietal lobe (Fig. 2).

Cell Transplantation

Animals were randomly assigned to the IA (n=12), IV (n= 12), SPIO (n=8), and control groups (n=8). Three days following photothrombotic infarction, rats allocated to the IA group received internal carotid artery injections of SPIO-labeled hBM-MSCs and the IV group received tail vein injections of SPIO-labeled hBM-MSCs. Rats assigned to the SPIO group received tail vein injections of 25 ug/mL of SPIO only and the control group received nothing after photothrombotic infarction (Table 1).

Rats were anesthetized before transplantation by intramuscular injection of a mixture of Ketara® (ketamine hydrochloride; Yuhan Corporation, Seoul, Korea) at 100 mg/kg and Rompun® (xylazine hydrochloride; Bayer Korea, Ltd.,

Ansan, Korea) at 10 mg/kg. In the IV group, 2.5×10⁵ cells/mL of SPIO-labeled hBM-MSCs were prepared in the medium, and slowly injected into the tail vein for 90 seconds with the 24-G needle (Introcane Celto; B. Braun Melsungen AG, Melsungen, Germany). For IA injections, the ipsilateral carotid artery was exposed, the external carotid artery was ligated with 6-0 silk, and 2.5×10⁵ cells/mL of SPIO-labeled hBM-MSCs were injected into the internal carotid artery through the common carotid artery using a 24-G needle. In the SPIO group, 25 ug/mL of SPIO were prepared in the medium, and slowly injected into the tail vein for 90 seconds with the 24-G needle.

In vitro cellular MRI

To determine the relationship between cell numbers and MRI signal intensities, *in vitro* cellular MRI was done. The SPIO-labeled hBM-MSCs were washed with PBS to remove unlabeled SPIO and treated with 0.25% trypsin-EDTA for 3 minutes. The labeled cells were counted and transferred to 0.5 mL tubes filled with normal saline, to provide cell counts of 6.3×10⁴, 1.3×10⁵, 2.5×10⁵, and 5.0×10⁵ cells, and centrifuged for 3 minutes at 12000 rpm to make pellets. Tubes containing 5×10⁵ cells/mL of unlabeled hBM-MSCs and 0.5 mL of normal saline without cells were also prepared as controls. MR imaging of phantoms was performed using a wrist coil (SENSE-wrist-4 channel; Philips, Eindhoven, the Netherlands) and 3T MRI (Philips, Eindhoven, the Netherlands) using T2-weighted (T2WI), T2*-weighted (T2*WI), and susceptibility-weighted (SWI) imaging.

Table 1. Table of study design with animal group

Groups	No. of cells	MRI (hrs)	Endpoint (hrs)	Specimen
IA				
1 hr	2.5×10 ⁵	Pre, 1	1	3
6 hr	2.5×10 ⁵	Pre, 1, 6	6	3
24 hr	2.5×10 ⁵	Pre, 1, 6, 24	24	3
48 hr	2.5×10 ⁵	Pre, 1, 6, 24, 48	48	3
IV				
1 hr	2.5×10 ⁵	Pre, 1	1	3
6 hr	2.5×10 ⁵	Pre, 1, 6	6	3
24 hr	2.5×10 ⁵	Pre, 1, 6, 24	24	3
48 hr	2.5×10 ⁵	Pre, 1, 6, 24, 48	48	3
SPIO				
1 hr	No, SPIO IV	Np	1	2
6 hr	No, SPIO IV	Np	6	2
24 hr	No, SPIO IV	Np	24	2
48 hr	No, SPIO IV	Pre, 1, 6, 24, 48	48	2
Control				
1 hr	No	Np	1	2
6 hr	No	Np	6	2
24 hr	No	Np	24	2
48 hr	No	Pre, 1, 6, 24, 48	48	2

IA : intra-arterial, IV : intravenous, SPIO : superparamagnetic iron oxide, pre : previous cell injection, 72 hrs after photothrombotic infarction, np : not performed, endpoint : sacrificed point after cell injection

For T2WI, the sequence parameters were repetition time (TR) 2706 msec, echo time (TE) 80 msec, flip angle 90°, field of view (FOV) 250×250 mm, matrix size 700×641, thickness 1 mm, gap 1 mm, and NEX 3. For T2*WI, sequence parameters were TR 525.9 msec, TE 9.2 msec, flip angle 30°, FOV 250×250 mm, matrix size 676×674, thickness 1 mm, gap 1 mm, and NEX 3. For SWI, sequence parameters were TR 35 msec, TE 45 msec, flip angle 10°, FOV 250×250 mm, matrix size 485×485, thickness 1 mm, and NEX 3.

MRI obtained at 6.3×10^4 , 1.3×10^5 , 2.5×10^5 and 5.0×10^5 cells showed that ferumoxide-labeling caused signals to become dark in a dose-dependent manner. Among the pulse sequences, SWI showed the maximum susceptibility effect of SPIO followed by T2*WI and T2WI. No significant susceptibility effect was noted in unlabeled hBM-MSCs or normal saline on MRI (Fig. 3).

In vivo MRI

For MRI, rats were anesthetized by intramuscular injection of a mixture of Ketara® at 100 mg/kg body weight and Rompun® at 10 mg/kg. Animals were imaged at 3 days after photothrombotic infarction (before cell transplantation), and at 1, 6, 24, and 48 hours after cell transplantation. The 3T MRI (Philips) and a wrist coil (SENSE-wrist-4 channel; Philips) were used. The brain MRI was taken with sequence parameters set for T2WI (TR 4279 msec, TE 80 msec, flip angle 90°, FOV 500×500 mm, matrix size 200×200, thickness 1 mm, gap 1 mm, and NEX 3), T2*WI (TR 719 msec, TE 23 msec, flip angle 18°, FOV 500×500 mm, matrix size 200×200, thickness 1 mm, gap 1 mm, and NEX 3), SWI (TR 31 msec, TE 44 msec, flip angle 15°, FOV

500×500 mm, matrix size 128×128, thickness 0.5 mm, and NEX 3), and diffusion weighted image (DWI : TR 4000 msec, TE 97 msec, flip angle 90°, FOV 500×500 mm, matrix size 64×55, thickness 1 mm, gap 1 mm, and NEX 4). The animal was placed in supine position.

We evaluated dark signal intensities in the infarcted regions after administration of the hBM-MSCs by IA and IV, and compared groups using the ImageJ program (from the U.S. National Institutes of Health, Bethesda, MD, USA) to quantify the dark spots in pixels.

Tissue preparation and pathology

Animals from each group were euthanized at 1, 6, 24, and 48 hours after cell transplantation. The brain of each animal was evaluated by counting transplanted cells in coronal brain sections stained with Prussian blue. Rats were anesthetized before sacrifice by intramuscular injection of a mixture of Ketara® at 100 mg/kg body weight and Rompun® at 10 mg/kg. Intracardial perfusion of ice-cold heparinized saline was followed by 4% paraformaldehyde perfusion. After removal of the brain and overnight postfixation, coronal sections were taken from rostral to caudal at 3-mm intervals. Coronal sections 5 μm thick were obtained from each block using a microtome (Leica Instruments, Leica Instrument, Heidelberg, Germany) and embedded in paraffin. To analyze the number of cells in the brain, two different sections at midline of the infarction were analyzed. All transplanted cells in the whole ipsilateral hemisphere of each section were counted. After removal and overnight postfixation of both the right upper and lower lobes of the lung, coronal sections of 5 μm were obtained from each block embedded in paraffin using a microtome. Cells were counted in randomly chosen sections from three different lobes of the lung.

Hematoxylin and eosin staining

Hematoxylin and eosin staining was performed for anatomic orientation and evaluation of tissue hemorrhage. Sections were fixed in 4% paraformaldehyde and immersed in a solution of xylene and ethanol for deparaffinization and rehydration. After washing briefly in distilled water, sections were stained in Harris hematoxylin solution for 8 minutes. The stained sections were washed in running tap water, rinsed in 95% ethanol and counterstained in eosin-phloxine solution for one minute.

Prussian blue staining

Prussian blue staining was performed in order to localize the iron particles in SPIO-labeled hBM-MSCs.

In vitro staining

The cells were washed twice with PBS to remove excess contrast agent (PLL-SPIO mixture), fixed with 4% paraformaldehyde, washed again and incubated with 2% potassium ferrocyanide (i.e., Perl's reagent) in 2% hydrochloric acid for 30 minutes.

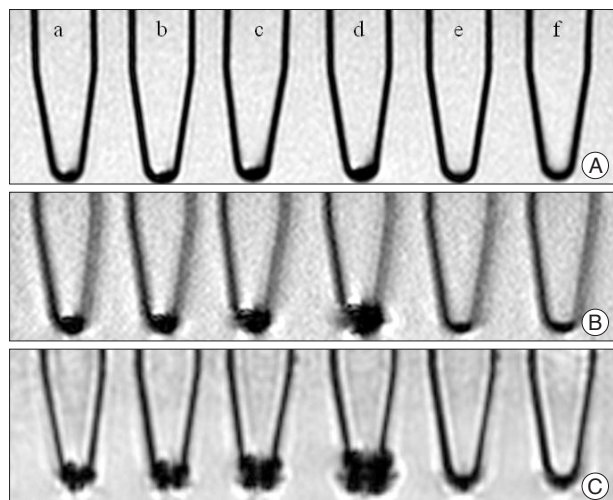


Fig. 3. *In vitro* cellular MRI of PBS phantoms containing suspensions of different concentrations of SPIO labeled hBM-MSCs. A : T2 weighted image. B : T2* weighted image (GRE). C : Susceptibility weighted image. (a) 6.3×10^4 cells/mL, (b) 1.3×10^5 cells/mL, (c) 2.5×10^5 cells/mL, (d) 5.0×10^5 cells/mL, (e) unlabeled hMSC 5.0×10^5 cells/mL, (f) no cells (normal saline). PBS : phosphate-buffered saline, hBM-MSCs : human bone marrow-derived mesenchymal stem cells, SPIO : superparamagnetic iron oxide, hMSC : human mesenchymal stem cell.

After three washes with dextrose water, the cells were counterstained with nuclear fast red.

***In vivo* staining**

The sections were washed twice with PBS to remove excess contrast agent, washed again and fixed with 4% paraformaldehyde. Sections were immersed in a solution of xylene and ethanol for deparaffinization and rehydration, and then incubated with 2% potassium ferrocyanide in 2% hydrochloric acid for 30 minutes. The sections were washed three times with dextrose water and counterstained with nuclear fast red.

Combined staining with anti-mitochondrial antibody and Prussian blue

Anti-human-mitochondrial antibody recognizes a 60 kDa nonglycosylated protein component of mitochondria found in human cells. It can be used to stain mitochondria in cells, tissues and biochemical preparations, and can be used as a mitochondrial marker in subcellular fractions. Combined staining with anti-mitochondrial antibody and Prussian blue was performed to co-localize mitochondria of human origin and iron particles in SPIO-labeled hBM-MSCs.

***In vitro* staining**

The cells were fixed with 4% paraformaldehyde. To detect antigen, cells were heated for 12 minutes in citrate buffer (pH 6.0) that had been preheated for 3 minutes. The cells were treated with 0.3% H₂O₂ for 10 minutes to remove endogenous peroxidase activity, washed with PBS and incubated overnight at 4°C with anti-mitochondrial antibody (clone 113-1, Chemicon, Temecula, CA, USA) as the primary antibody. After washing with PBS, the cells were treated with secondary antibody (EnVision System-HRP; Dako, Copenhagen, Denmark) for 30 minutes at room temperature. Immunoreactivity was visualized with a diaminobenzidine tetrachloride kit (Dako, Copenhagen, Denmark) using a treatment time of 1-5 minutes. Prussian blue staining was performed as described above.

***In vivo* staining**

After fixation in 4% paraformaldehyde, sections were immersed in a xylene and ethanol solution for deparaffinization and rehydration. To detect tissue antigen, the sections were heated for 12 minutes in citrate buffer (pH 6.0) that had been preheated for 3 minutes. The specimens were treated with 0.3% H₂O₂ for 10 minutes to remove endogenous peroxidase activity, washed with PBS and incubated overnight at 4°C with anti-mitochondrial antibody as the primary antibody (clone 113-1, Chemicon). After washing with PBS, the specimens were treated with secondary antibody (EnVision System-HRP; Dako) for 30 minutes at room temperature. Immunoreactivity was visualized by treatment with diaminobenzidine tetrachloride for 1-5 minutes. Prussian blue staining was performed as described above.

Statistical analysis

Pixel counts from the brain MRI and engrafted-cell counts from pathological analysis of brain and lung were compared between the IA and IV groups using analysis of variance followed by the Mann-Whitney test. Data are presented as means±SE. The significance level was set at 0.05.

RESULTS

***In vivo* MRI**

On MRI, the brain infarction presented high signal intensity on T2WI. On T2WI, T2*WI, and SWI, grafted cells appeared as dark signal intensity at the ischemic boundary. In the IA group, dark signal intensity in the zone surrounding the infarction increased substantially over time. SWI showed largest dark signal intensity regions followed by T2*WI and T2WI in all groups. In the IV group, dark signal intensity were also observed in the peri-lesional zone but were less prominent than in corresponding images from the IA group. Distributions of dark signal intensities in peri-lesional zones were similar in both IA and IV groups (Fig. 4). Linear parenchymal low-signal intensities suggestive of veins were noted in all groups on SWI. On T2WI and DWI, a high signal intensity lesion was seen in deep gray matter of brain suggestive of acute infarction and probably caused by a cluster of cells. On SWI the pixel counts of dark signal intensity in the peri-lesional zone were significantly larger in groups that received IA administration ($p < 0.05$). Mean dark signal intensity pixel numbers of 478.6±9.0, 570.4±22.2, 789.7±21.1, and 722.5±9.3 were detected in the brain at 1, 6, 24, and 48 hours, respectively, after IA injection vs. 205.3±20.7, 240.7±11.1, 374.2±28, and 380.8±38.5 after IV (Fig. 5).

Pathology of brain

Prussian blue staining

Intravascular transplantation of SPIO-labeled hBM-MSCs in this photothrombotic model resulted in cerebral engraftment detected by Prussian blue staining. The distribution of transplanted cells varied in different cerebral regions. The highest cell density was detected in the peri-lesional zone, although some cells were detected at distances from the infarction. The dark signal intensity regions observed on MRI were found to correspond to grafted regions as determined by Prussian blue staining (Fig. 6A, B). Counting of SPIO-labeled hBM-MSCs showed that significantly greater numbers of cells were engrafted at 48 hours in groups treated by IA administration ($p < 0.05$) (Fig. 6C). At 48 hours after IA injection, the mean cell number observed within the cerebrum was 52.8 as compared to 25.4 after IV. At 1, 6, and 24 hours, only rare transplanted cells were observed in either the IA or IV groups. Mean cell numbers of 5.8, 7.2, and 8.3, respectively, were detected within the brain at these times after IA injection vs. 1.0, 1.8, and 3.3 after IV, but these differences between IA and IV groups were not significant. In both

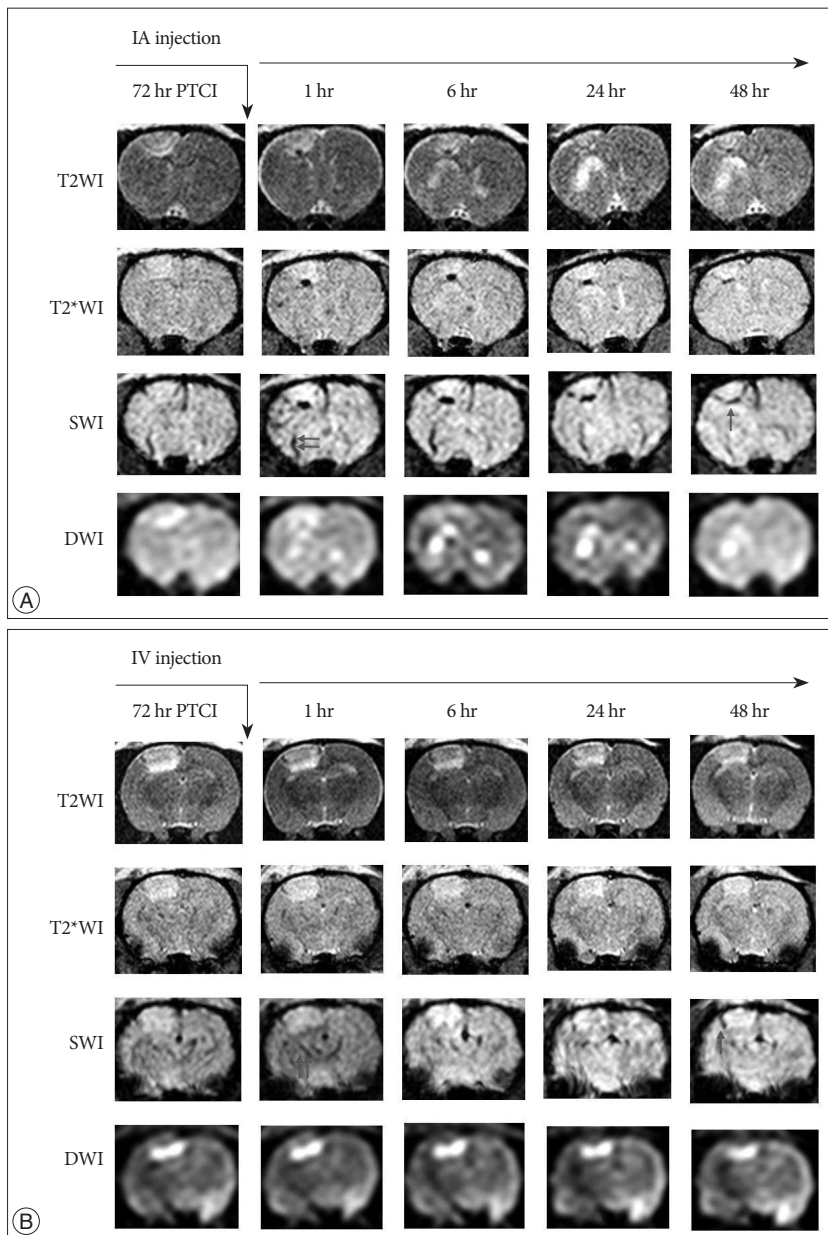


Fig. 4. Serial brain MRI after regions IA (A) and IV (B) administration after photothrombotic infarction of rat model. Acute infarction are located on the right side of the brain (the left side of the images). Dark signal intensity regions increased over time especially in peripheral portion of infarction. SWI shows largest dark signal intensity regions following T2*WI and T2WI (arrows). Linear parenchymal low-signal intensities suggestive of veins are noted in all groups on SWI (double arrows). In the IA group, dark signal intensity in peripheral portion of infarction are more prominent than in corresponding images from a the IV group. PTCI : photothrombotic cerebral infarction, IA : intra-arterial, IV : intravenous, T2*WI : T2* weighted image, T2WI : T2 weighted image, SWI : susceptibility weighted image, DWI : diffusion weighted image.

groups, cell engraftments at 48 hours was significantly superior than those at one hour after cell infusion ($p < 0.05$). Engrafted cells were not detected in SPIO and control groups.

Combined staining with anti-mitochondrial antibody and Prussian blue

Intravascular transplantation of labeled hBM-MSC in this

photothrombotic model resulted in cerebral engraftment as detected by combined anti-mitochondrial antibody and Prussian blue staining (Fig. 6D). The highest cell density was detected in the peri-lesional zone.

Pathology of the lung

Prussian blue staining analysis of the lung showed that hBM-MSC entrapment were significantly larger in the IV group than in the IA group at 1 hour time point ($p < 0.05$) (Fig. 7). Mean cell numbers of 5.7 and 1.0 were detected within lung parenchyma after IV and IA injection, respectively, at 1 hour. This was a first-pass effect, in that no trend was observed in the groups at 6, 24, 48 hours.

DISCUSSION

In this study, we compared the selectivity of IA and IV in transplantation of stem cells to the brain in a rat photothrombotic model of ischemic stroke. Quantitative analysis by MRI at all time points and by pathology at 48 hours showed that IA transplantation was significantly more effective than IV. At 1, 6, 24 hours, we observed a trend toward a larger number of engrafted cells in the IA groups as compared to the IV groups. Analysis of the lung showed a first passage effect that resulted in significantly greater engraftment of cells by IV than by IA administration at 1 hour. The IA route showed greater effectiveness for specific delivery of stem cells to the brain following acute infarction.

There was difference in time distribution of stem cells between MRI and histological analysis. On MRI study, the peak mean pixel number of dark signal was noted at 24 hours in IA group, and at 48 hours in IV group. However, on histological analysis, the peak cell count was seen at 48 hours both in IA and IV groups. This could be explained by perilesional hemorrhage of photothrombotic model in IA group which resulted in false outcome in 24 hour IA group, but could not be identified on histological specimen. We think the peak time of stem cell arrival is actually similar in IA and IV group, and the main cause of cell count difference between two groups is pulmonary circulation (first passage effect).

A common characteristic of ischemic stroke is the inflammatory response, with recruitment of leukocytes to the site of injury^{24,60}. Ischemia results in activation of the endothelium, and of chemokine-producing astrocytes and microglia. Inflammatory cytokines [e.g., vascular cell adhesion molecule-1, intercellular adhesion molecule-1, C-C chemokine ligands (CCL)2, CCL3, CCL4, CCL5, and C-X-C motif ligand 12a] increase vascular permeability and may thereby facilitate stem cell engraftment^{24,50}. Stem cells, like leukocytes, express integrins such as CD49d and the chemokine receptors such as chemokine receptors CCR1, CCR2, CCR5, CXCR3, and CXCR4^{49,58}. Various types of stem cells may use extravasation mechanisms to those of immune cells, such as adhesion, chemoattraction, and transendothelial migration^{3,49}. Well known pairs of cytokine ligand/cytokine receptor are vascular cell adhesion molecule-1/CD49d, CCL2/CCR2, and SDF-1/CXCR4^{3,27,61}.

Functional recovery may be achieved through various routes of MSC administration, including intracerebral, IA, and IV^{13,15,18,26,34,55,59}. Intracerebral and intravascular administration provide the best chance to engraft MSCs to the brain. Intravascular delivery is less invasive than intracerebral stereotactic delivery. In the field of experimental endovascular transplantation, IV infusion has been tested more extensively than IA administration. However, recent studies have demonstrated an unfavorable distribution of cells after IV infusion^{38,42,48}. One study using bioluminescence imaging (BLI) of neural stem cells after middle cerebral artery occlusion (MCAO) showed a BLI signal from the brain that was 12 times higher in IA-injected than in IV-injected animals. After IA injection, 69% of the total luciferase activity emerged from the brain early after transplantation and 93% at 1 week. After intravenous injection, 94% of the BLI signal was detected in the lungs followed by an overall signal loss of 94% at 1 week; thus the cells failed to survive outside the brain⁴⁸. Another study using immunohistochemical analysis of engrafted MSCs transplanted after brain injury detected a significantly higher number of transplanted MSCs in the injured brain after IA as compared to IV administration at both 1 day and day 5 after transplantation⁴². Use of Prussian blue staining and MRI of labeled neural progenitor cells after MCAO showed significantly greater cell migration, wider distribution, and a larger number of transplanted neural progenitor cells in the target brain area following IA administration than by IV or intracisternal administration³⁸. The majority of administered MSCs are ini-

tially trapped in the pulmonary capillaries and removed from circulation in the first passage effect^{22,47}. The first passage effect in lung differs significantly between IA and IV administration. Cells administered by IA generate higher local concentrations, have shorter blood stream exposure, and suffer less mechanical stress before reaching the target site⁴². In agreement with the previous studies, we found significantly more stem cells residing in the brain after IA administration than with the IV route and higher total entrapment of cells in the lung after IV as compared

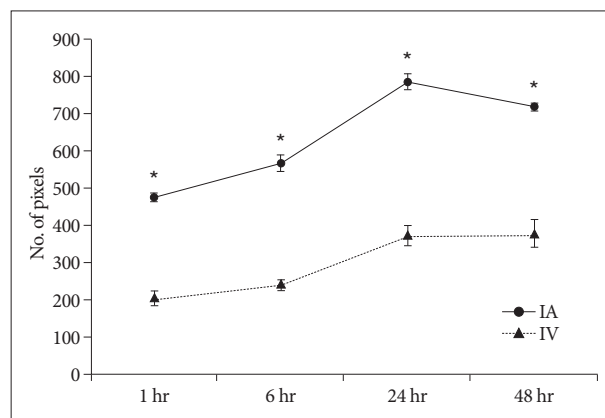


Fig. 5. Quantitative analysis of MRI. Graph depicting mean (\pm SE) number of pixel count of dark signal intensity on SWI after either selective intra-arterial (IA) or intravenous (IV) transplantation in a rat model of photothrombotic infarction ($*p < 0.05$). SWI : susceptibility weighted image.

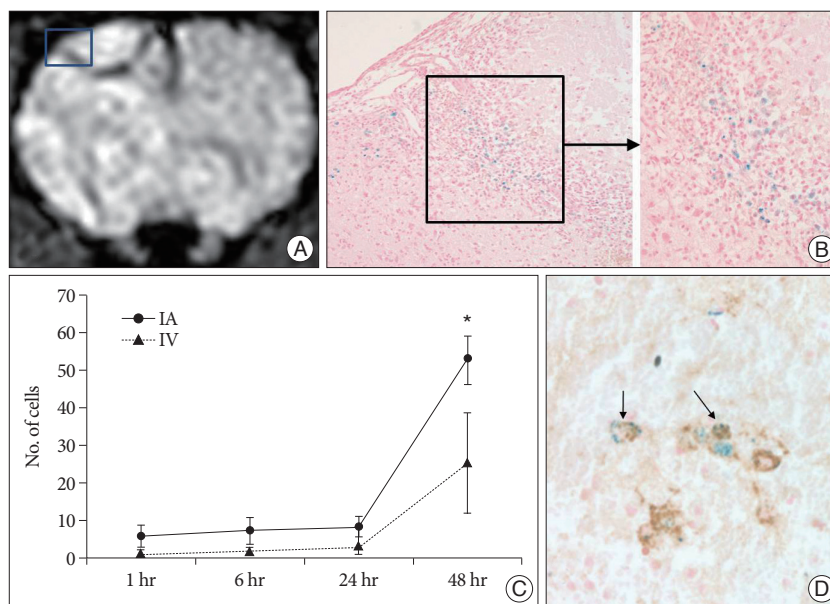


Fig. 6. MRI of rat brain (IA 48 hr), SPIO-labeled hBM-MSCs directly grafted into a rat brain, and Prussian blue-stained cells and antimitochondrial-Prussian blue stained cells in a rat brain. A : Implanted cells are visualized as low signal intensity on SWI of MRI. B : Hypointense areas [square in (A)] represent massive invasions by Prussian blue stained cells (original magnification $\times 200$, $\times 400$). C : Graph showing the mean (\pm SE) number of engrafted cells in brain after either selective IA or IV transplantation ($*p < 0.05$). D : Among these cells antimitochondrial-Prussian blue stained cells are noted (arrows, original magnification $\times 400$). IA : intra-arterial, IV : intravenous, SPIO : superparamagnetic iron oxide, SWI : susceptibility weighted image, hBM-MSCs : human bone marrow-derived mesenchymal stem cells.

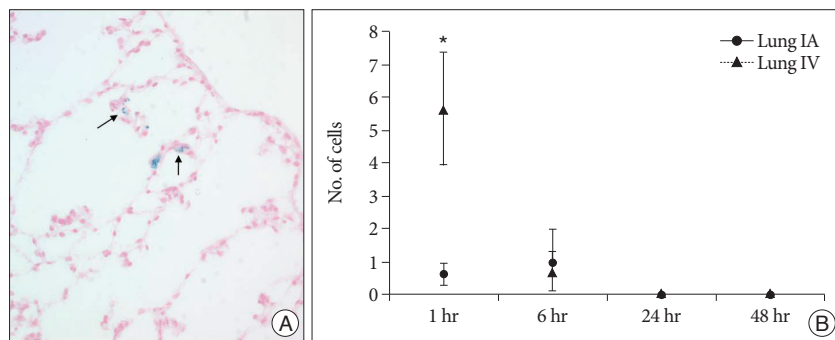


Fig. 7. Prussian blue-stained cells in lung specimen and graph showing the mean (\pm SE) number of engrafted cells after either selective intra-arterial (IA) or intravenous (IV) transplantation. A : Several Prussian blue-stained cells are noted in alveolar wall (arrows, original magnification \times 400). B : hBM-MSC entrapment were significantly larger in the IV group than in the IA group at 1 hour time point ($*p < 0.05$). hBM-MSCs : human bone marrow-derived mesenchymal stem cells.

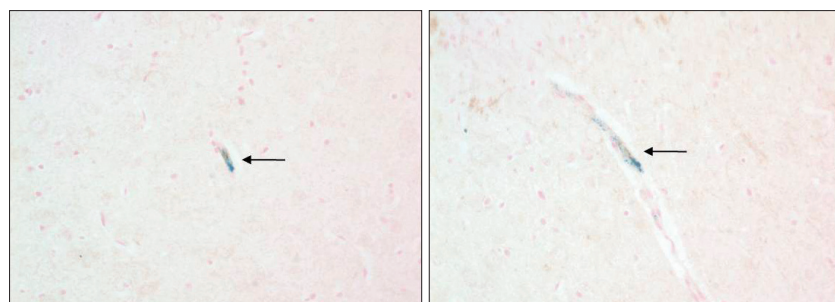


Fig. 8. Aggregated MSCs at arterial lumen in IA rat model on combined Anti-mitochondrial antibody-Prussian blue staining. Note aggregated cells (arrows) which are positive on Anti-mitochondrial antibody (brown color) and Prussian blue staining (blue color).

to IA administration. However, more animals were assigned to the IA group than to the IV group, because carotid artery injection resulted in high mortality, possibly through distal embolization of intraluminal plaques^{38,59}. Several rat treated by IA in the present study showed MSC aggregates in the arterial lumen on combined staining with anti-mitochondrial antibody and Prussian blue (Fig. 8). These findings suggested that intracarotid infusion may cause further ischemia or thrombosis in humans. In this respect, the intravenous infusion of MSCs may prove to be the safer and more feasible route for stem cell therapy in stroke patients^{6,31,36}.

Cerebral ischemia is induced experimentally by transient or permanent occlusion of the middle cerebral artery (MCA) with an intraluminal filament^{19,34}. But this MCAO model requires delicate microsurgical skills and the size of the infarction is highly dependent on the vascular anatomy of the MCA and collateral vessels⁴⁵. In addition, the size of infarction corresponding to the MCA territory and the resulting neurologic deficits are too extensive for use to study a healing process³⁴. Cortical focal photothrombosis in the brain is a well-established model of stroke that uses photosensitive dyes such as Rose Bengal⁶². Light-activated Rose Bengal induces free-radical injury to endothelial cells, aggregation of platelets and finally occlusion of the injured vessel. Advantages of the Rose Bengal photothrombotic model included the non-invasiveness of the operation and resulting lesions of re-

producable size with well-defined boundaries between the infarct and normal tissues^{11,35,64}. Unlike the MCAO model, which showed a diffuse stem cell distribution by IA infusion and a localized pattern by IV infusion³⁸, the photothrombotic infarction model showed similar patterns of stem cell distribution following IA and IV infusions, in the peripheral zone of the infarction.

The value of MRI in monitoring and tracking stem cells injected into the brain is established with various cell types, including MSCs³⁰, neural progenitor cells³⁸, myogenic precursors²⁵, and embryonic stem cells⁵. SPIO nanoparticles provide the most sensitive markers for labeling stem cells for MRI¹². SWI is the most sensitive MRI pulse sequence for detecting iron content in the brain. SWI exploits the magnetic susceptibility differences between tissues⁵². The SWI technique uses a fully velocity-compensated, RF spoiled, high-resolution, 3-D modified gradient-echo T2*-weighted sequence^{28,53,54} that accurately presents the iron content, paramagnetic blood products, and the venous vasculature in

the brain^{2,52}.

We are aware of limitations in our study. First, the number of animals in each group was relatively small. It is possible that with larger numbers the differences between IA and IV groups would have been more significant. Second, we used hBM-MSCs in immunocompetent rats. It may cause that the engrafted MSCs will be targeted by immune cells and decrease the survival rate of cells. Third, sensitivity of MRI in detecting magnetically labeled cells is affected by various factors, including the magnetic field strength of the MR instrument and the MR imaging software⁴⁴. Therefore, our imaging measurements at 3T may have lacked the sensitivity to detect small numbers of cells or tiny cell clusters that migrated into the host brain. Fourth, photothrombotic infarct model may cause perilesional hemorrhage which mimics SPIO containing stem cells on MRI. As a result, our data may have shown difference in time distribution of stem cells between MRI and histological analysis.

CONCLUSION

In a rat photothrombotic model of ischemic stroke, selective intra-arterial administration of human mesenchymal stem cells is more effective than intravenous administration. MRI and pathologic analyses revealed the time course of cell migration, and the numbers and distribution of hBM-MSCs delivered into

the brain. Intra-arterial endovascular procedure could be a novel way in the stem cell treatment of cerebral infarction.

References

- Abdallah BM, Haack-Sørensen M, Burns JS, Elsnab B, Jakob F, Hokland P, et al. : Maintenance of differentiation potential of human bone marrow mesenchymal stem cells immortalized by human telomerase reverse transcriptase gene despite [corrected] extensive proliferation. *Biochem Biophys Res Commun* 326 : 527-538, 2005
- Akter M, Hirai T, Hiai Y, Kitajima M, Komi M, Murakami R, et al. : Detection of hemorrhagic hypotense foci in the brain on susceptibility-weighted imaging clinical and phantom studies. *Acad Radiol* 14 : 1011-1019, 2007
- Andres RH, Choi R, Pendharker AV, Gaeta X, Wang N, Nathan JK, et al. : The CCR2/CCL2 interaction mediates the transendothelial recruitment of intravascularly delivered neural stem cells to the ischemic brain. *Stroke* 42 : 2923-2931, 2011
- Andres RH, Choi R, Steinberg GK, Guzman R : Potential of adult neural stem cells in stroke therapy. *Regen Med* 3 : 893-905, 2008
- Arai T, Kofidis T, Bulte JW, de Bruin J, Venook RD, Berry GJ, et al. : Dual in vivo magnetic resonance evaluation of magnetically labeled mouse embryonic stem cells and cardiac function at 1.5 t. *Magn Reson Med* 55 : 203-209, 2006
- Bang OY, Lee JS, Lee PH, Lee G : Autologous mesenchymal stem cell transplantation in stroke patients. *Ann Neurol* 57 : 874-882, 2005
- Barry FP, Murphy JM : Mesenchymal stem cells : clinical applications and biological characterization. *Int J Biochem Cell Biol* 36 : 568-584, 2004
- Borlongan CV, Lind JG, Dillon-Carter O, Yu G, Hadman M, Cheng C, et al. : Bone marrow grafts restore cerebral blood flow and blood brain barrier in stroke rats. *Brain Res* 1010 : 108-116, 2004
- Borlongan CV, Lind JG, Dillon-Carter O, Yu G, Hadman M, Cheng C, et al. : Intracerebral xenografts of mouse bone marrow cells in adult rats facilitate restoration of cerebral blood flow and blood-brain barrier. *Brain Res* 1009 : 26-33, 2004
- Brazelton TR, Rossi FM, Keshet GI, Blau HM : From marrow to brain : expression of neuronal phenotypes in adult mice. *Science* 290 : 1775-1779, 2000
- Buchkremer-Ratzmann I, August M, Hagemann G, Witte OW : Electrophysiological transcortical diaschisis after cortical photothrombosis in rat brain. *Stroke* 27 : 1105-1109; discussion 1109-1111, 1996
- Bulte JW, Kraitchman DL : Monitoring cell therapy using iron oxide MR contrast agents. *Curr Pharm Biotechnol* 5 : 567-584, 2004
- Chen J, Li Y, Katakowski M, Chen X, Wang L, Lu D, et al. : Intravenous bone marrow stromal cell therapy reduces apoptosis and promotes endogenous cell proliferation after stroke in female rat. *J Neurosci Res* 73 : 778-786, 2003
- Chen J, Li Y, Wang L, Lu M, Zhang X, Chopp M : Therapeutic benefit of intracerebral transplantation of bone marrow stromal cells after cerebral ischemia in rats. *J Neurol Sci* 189 : 49-57, 2001
- Chen J, Zhang ZG, Li Y, Wang L, Xu YX, Gautam SC, et al. : Intravenous administration of human bone marrow stromal cells induces angiogenesis in the ischemic boundary zone after stroke in rats. *Circ Res* 92 : 692-699, 2003
- Chen X, Li Y, Wang L, Katakowski M, Zhang L, Chen J, et al. : Ischemic rat brain extracts induce human marrow stromal cell growth factor production. *Neuropathology* 22 : 275-279, 2002
- Chopp M, Li Y : Treatment of neural injury with marrow stromal cells. *Lancet Neurol* 1 : 92-100, 2002
- Chu K, Kim M, Park KI, Jeong SW, Park HK, Jung KH, et al. : Human neural stem cells improve sensorimotor deficits in the adult rat brain with experimental focal ischemia. *Brain Res* 1016 : 145-153, 2004
- Clark WM, Lessov NS, Dixon MP, Eckenstein F : Monofilament intraluminal middle cerebral artery occlusion in the mouse. *Neurol Res* 19 : 641-648, 1997
- Cui X, Chen J, Zacharek A, Li Y, Roberts C, Kapke A, et al. : Nitric oxide donor upregulation of stromal cell-derived factor-1/chemokine (CXC motif) receptor 4 enhances bone marrow stromal cell migration into ischemic brain after stroke. *Stem Cells* 25 : 2777-2785, 2007
- Dezawa M, Kanno H, Hoshino M, Cho H, Matsumoto N, Itokazu Y, et al. : Specific induction of neuronal cells from bone marrow stromal cells and application for autologous transplantation. *J Clin Invest* 113 : 1701-1710, 2004
- Fischer UM, Harting MT, Jimenez F, Monzon-Posadas WO, Xue H, Savitz SI, et al. : Pulmonary passage is a major obstacle for intravenous stem cell delivery : the pulmonary first-pass effect. *Stem Cells Dev* 18 : 683-692, 2009
- Friedenstein AJ, Chailakhjan RK, Lalykina KS : The development of fibroblast colonies in monolayer cultures of guinea-pig bone marrow and spleen cells. *Cell Tissue Kinet* 3 : 393-403, 1970
- Frijns CJ, Kappelle LJ : Inflammatory cell adhesion molecules in ischemic cerebrovascular disease. *Stroke* 33 : 2115-2122, 2002
- Garot J, Unterseh T, Teiger E, Champagne S, Chazaud B, Gherardi R, et al. : Magnetic resonance imaging of targeted catheter-based implantation of myogenic precursor cells into infarcted left ventricular myocardium. *J Am Coll Cardiol* 41 : 1841-1846, 2003
- Guzman R, Choi R, Gera A, De Los Angeles A, Andres RH, Steinberg GK : Intravascular cell replacement therapy for stroke. *Neurosurg Focus* 24 : E15, 2008
- Guzman R, De Los Angeles A, Cheshier S, Choi R, Hoang S, Liauw J, et al. : Intracarotid injection of fluorescence activated cell-sorted CD49d-positive neural stem cells improves targeted cell delivery and behavior after stroke in a mouse stroke model. *Stroke* 39 : 1300-1306, 2008
- Haacke EM, Xu Y, Cheng YC, Reichenbach JR : Susceptibility weighted imaging (SWI). *Magn Reson Med* 52 : 612-618, 2004
- Hicks A, Jolkonen J : Challenges and possibilities of intravascular cell therapy in stroke. *Acta Neurobiol Exp (Wars)* 69 : 1-11, 2009
- Hill JM, Dick AJ, Raman VK, Thompson RB, Yu ZX, Hinds KA, et al. : Serial cardiac magnetic resonance imaging of injected mesenchymal stem cells. *Circulation* 108 : 1009-1014, 2003
- Honmou O, Houkin K, Matsunaga T, Niitsu Y, Ishiai S, Onodera R, et al. : Intravenous administration of auto serum-expanded autologous mesenchymal stem cells in stroke. *Brain* 134 (Pt 6) : 1790-1807, 2011
- Jin K, Sun Y, Xie L, Mao XO, Childs J, Peel A, et al. : Comparison of ischemia-directed migration of neural precursor cells after intrastriatal, intraventricular, or intravenous transplantation in the rat. *Neurobiol Dis* 18 : 366-374, 2005
- Kassem M : Mesenchymal stem cells : biological characteristics and potential clinical applications. *Cloning Stem Cells* 6 : 369-374, 2004
- Kitagawa K, Matsumoto M, Yang G, Mabuchi T, Yagita Y, Hori M, et al. : Cerebral ischemia after bilateral carotid artery occlusion and intraluminal suture occlusion in mice : evaluation of the patency of the posterior communicating artery. *J Cereb Blood Flow Metab* 18 : 570-579, 1998
- Lee JK, Park MS, Kim YS, Moon KS, Joo SP, Kim TS, et al. : Photochemically induced cerebral ischemia in a mouse model. *Surg Neurol* 67 : 620-625; discussion 625, 2007
- Lee JS, Hong JM, Moon GJ, Lee PH, Ahn YH, Bang OY; STARTING collaborators : A long-term follow-up study of intravenous autologous mesenchymal stem cell transplantation in patients with ischemic stroke. *Stem Cells* 28 : 1099-1106, 2010
- Leor J, Rozen L, Zulloff-Shani A, Feinberg MS, Amsalem Y, Barbash IM, et al. : Ex vivo activated human macrophages improve healing, remodeling, and function of the infarcted heart. *Circulation* 114 (1 Suppl) :

- I94-I100, 2006
38. Li L, Jiang Q, Ding G, Zhang L, Zhang ZG, Li Q, et al. : Effects of administration route on migration and distribution of neural progenitor cells transplanted into rats with focal cerebral ischemia, an MRI study. *J Cereb Blood Flow Metab* 30 : 653-662, 2010
 39. Li Y, Chen J, Chen XG, Wang L, Gautam SC, Xu YX, et al. : Human marrow stromal cell therapy for stroke in rat : neurotrophins and functional recovery. *Neurology* 59 : 514-523, 2002
 40. Li Y, Chen J, Zhang CL, Wang L, Lu D, Katakowski M, et al. : Gliosis and brain remodeling after treatment of stroke in rats with marrow stromal cells. *Glia* 49 : 407-417, 2005
 41. Liu W, Jiang X, Fu X, Cui S, Du M, Cai Y, et al. : Bone marrow stromal cells can be delivered to the site of traumatic brain injury via intrathecal transplantation in rabbits. *Neurosci Lett* 434 : 160-164, 2008
 42. Lundberg J, Le Blanc K, Söderman M, Andersson T, Holmin S : Endovascular transplantation of stem cells to the injured rat CNS. *Neuroradiology* 51 : 661-667, 2009
 43. Luria EA, Panasyuk AF, Friedenstein AY : Fibroblast colony formation from monolayer cultures of blood cells. *Transfusion* 11 : 345-349, 1971
 44. Magnitsky S, Watson DJ, Walton RM, Pickup S, Bulte JW, Wolfe JH, et al. : In vivo and ex vivo MRI detection of localized and disseminated neural stem cell grafts in the mouse brain. *Neuroimage* 26 : 744-754, 2005
 45. McAuley MA : Rodent models of focal ischemia. *Cerebrovasc Brain Metab Rev* 7 : 153-180, 1995
 46. Mezey E, Chandross KJ, Harta G, Maki RA, McKecher SR : Turning blood into brain : cells bearing neuronal antigens generated in vivo from bone marrow. *Science* 290 : 1779-1782, 2000
 47. Parr AM, Tator CH, Keating A : Bone marrow-derived mesenchymal stromal cells for the repair of central nervous system injury. *Bone Marrow Transplant* 40 : 609-619, 2007
 48. Pendharkar AV, Chua JY, Andres RH, Wang N, Gaeta X, Wang H, et al. : Biodistribution of neural stem cells after intravascular therapy for hypoxic-ischemia. *Stroke* 41 : 2064-2070, 2010
 49. Pluchino S, Zanotti L, Rossi B, Brambilla E, Ottoboni L, Salani G, et al. : Neurosphere-derived multipotent precursors promote neuroprotection by an immunomodulatory mechanism. *Nature* 436 : 266-271, 2005
 50. Rebenko-Moll NM, Liu L, Cardona A, Ransohoff RM : Chemokines, mononuclear cells and the nervous system : heaven (or hell) is in the details. *Curr Opin Immunol* 18 : 683-689, 2006
 51. Reddy AM, Kwak BK, Shim HJ, Ahn C, Cho SH, Kim BJ, et al. : Functional characterization of mesenchymal stem cells labeled with a novel PVP-coated superparamagnetic iron oxide. *Contrast Media Mol Imaging* 4 : 118-126, 2009
 52. Reichenbach JR, Venkatesan R, Schillinger DJ, Kido DK, Haacke EM : Small vessels in the human brain : MR venography with deoxyhemoglobin as an intrinsic contrast agent. *Radiology* 204 : 272-277, 1997
 53. Sehgal V, Delproposto Z, Haacke EM, Tong KA, Wycliffe N, Kido DK, et al. : Clinical applications of neuroimaging with susceptibility-weighted imaging. *J Magn Reson Imaging* 22 : 439-450, 2005
 54. Sehgal V, Delproposto Z, Haddad D, Haacke EM, Sloan AE, Zamorano LJ, et al. : Susceptibility-weighted imaging to visualize blood products and improve tumor contrast in the study of brain masses. *J Magn Reson Imaging* 24 : 41-51, 2006
 55. Shen LH, Li Y, Chen J, Zacharek A, Gao Q, Kapke A, et al. : Therapeutic benefit of bone marrow stromal cells administered 1 month after stroke. *J Cereb Blood Flow Metab* 27 : 6-13, 2007
 56. Shen LH, Li Y, Chen J, Zhang J, Vanguri P, Borneman J, et al. : Intracortical transplantation of bone marrow stromal cells increases axon-myelin remodeling after stroke. *Neuroscience* 137 : 393-399, 2006
 57. Shichinohe H, Kuroda S, Yano S, Ohnishi T, Tamagami H, Hida K, et al. : Improved expression of gamma-aminobutyric acid receptor in mice with cerebral infarct and transplanted bone marrow stromal cells : an autoradiographic and histologic analysis. *J Nucl Med* 47 : 486-491, 2006
 58. Tran PB, Ren D, Veldhouse TJ, Miller RJ : Chemokine receptors are expressed widely by embryonic and adult neural progenitor cells. *J Neurosci Res* 76 : 20-34, 2004
 59. Walczak P, Zhang J, Gilad AA, Kedziorek DA, Ruiz-Cabello J, Young RG, et al. : Dual-modality monitoring of targeted intraarterial delivery of mesenchymal stem cells after transient ischemia. *Stroke* 39 : 1569-1574, 2008
 60. Wang Q, Tang XN, Yenari MA : The inflammatory response in stroke. *J Neuroimmunol* 184 : 53-68, 2007
 61. Wang Y, Deng Y, Zhou GQ : SDF-1alpha/CXCR4-mediated migration of systemically transplanted bone marrow stromal cells towards ischemic brain lesion in a rat model. *Brain Res* 1195 : 104-112, 2008
 62. Watson BD, Dietrich WD, Busto R, Wachtel MS, Ginsberg MD : Induction of reproducible brain infarction by photochemically initiated thrombosis. *Ann Neurol* 17 : 497-504, 1985
 63. Wislet-Gendebien S, Hans G, Leprince P, Rigo JM, Moonen G, Rogister B : Plasticity of cultured mesenchymal stem cells : switch from nestin-positive to excitable neuron-like phenotype. *Stem Cells* 23 : 392-402, 2005
 64. Witte OW, Stoll G : Delayed and remote effects of focal cortical infarctions : secondary damage and reactive plasticity. *Adv Neurol* 73 : 207-227, 1997
 65. Woodbury D, Schwarz EJ, Prockop DJ, Black IB : Adult rat and human bone marrow stromal cells differentiate into neurons. *J Neurosci Res* 61 : 364-370, 2000
 66. Yang M, Wei X, Li J, Heine LA, Rosenwasser R, Iacovitti L : Changes in host blood factors and brain glia accompanying the functional recovery after systemic administration of bone marrow stem cells in ischemic stroke rats. *Cell Transplant* 19 : 1073-1084, 2010
 67. Zhu J, Zhou Z, Liu Y, Zheng J : Fractalkine and CX3CR1 are involved in the migration of intravenously grafted human bone marrow stromal cells toward ischemic brain lesion in rats. *Brain Res* 1287 : 173-183, 2009